

Enhancing Sparsity and Resolution via Reweighted Atomic Norm Minimization

Zai Yang and Lihua Xie, *Fellow, IEEE*

Abstract—The mathematical theory of super-resolution developed recently by Candès and Fernandes-Granda states that a continuous, sparse frequency spectrum can be recovered with infinite precision via a (convex) atomic norm technique given a set of regularly spaced time-space samples. This theory was then extended to the cases with partial/compressive samples and/or multiple measurement vectors via atomic norm minimization (ANM), known as off-grid/continuous compressed sensing. However, a major problem of existing atomic norm methods is that the frequencies can be recovered only if they are sufficiently separated, prohibiting commonly known high resolution. In this paper, a novel nonconvex optimization method is proposed which guarantees exact recovery under no resolution limit and hence achieves high resolution. A locally convergent iterative algorithm is implemented to solve the nonconvex problem. The algorithm iteratively carries out ANM with a sound reweighting strategy which enhances sparsity and resolution, and is termed as reweighted atomic-norm minimization (RAM). Extensive numerical simulations are carried out to demonstrate the performance of the proposed method with application to direction of arrival (DOA) estimation.

Index Terms—Continuous compressed sensing (CCS), DOA estimation, frequency estimation, gridless sparse method, high resolution, reweighted atomic norm minimization (RAM).

I. INTRODUCTION

Compressed sensing (CS) [1], [2] refers to a technique of reconstructing a high dimensional signal from far fewer samples and has brought significant impact on signal processing and information theory in the past decade. In conventional wisdom, the signal of interest needs to be sparse under a finite discrete dictionary for successful reconstruction, which limits its applications, for example, to array processing, radar and sonar, where the dictionary is typically specified by one or more continuous parameters. In this paper, we are concerned about a compressed sensing problem with a continuous dictionary which arises in line spectral estimation and array processing [3], [4]. In particular, we are interested in recovering L discrete sinusoidal signals which compose the data matrix $\mathbf{Y}^o \in \mathbb{C}^{N \times L}$ with its (j, t) th element (corrupted by noise in practice)

$$y_{jt}^o = \sum_{k=1}^K s_{kt} e^{i2\pi(j-1)f_k}, \quad (j, t) \in [N] \times [L], \quad (1)$$

where $i = \sqrt{-1}$, $f_k \in \mathbb{T} \triangleq [0, 1]$, $s_{kt} \in \mathbb{C}$ and $[N] = \{1, 2, \dots, N\}$. That is, each column of \mathbf{Y}^o is superimposed by K discrete sinusoids with frequencies $\{f_k\}$ and amplitudes $\{s_{kt}\}$. To recover \mathbf{Y}^o (and the frequency components in most

applications), however, we are only given partial/compressive samples on its rows indexed by $\Omega \subset [N]$ (of size $M < N$), denoted by \mathbf{Y}_Ω^o . This problem is referred to as off-grid or continuous compressed sensing (CCS) according to [5], [6] differing from existing CS framework in the sense that every frequency f_k can take any continuous value in \mathbb{T} rather than constrained on a finite discrete grid. The CCS problem with $L = 1$ or in the single-measurement-vector (SMV) case is usually known as line spectral estimation, where the compressive data issue can be deliberately implemented for efficient sampling and energy saving or accidentally caused by missing samples due to adversary environmental effects. The multiple-measurement-vector (MMV) case where $L > 1$ is common in array processing. Therein the sampling index set Ω refers to sensor placement of a linear sensor array and a smaller sample size means use of less sensors. \mathbf{Y}_Ω^o consists of measurements of the sensor array and each column vector corresponds to one data snapshot. Each frequency component corresponds to one source and its value determines the source direction. Consequently, the frequency estimation problem in CCS given the measurement matrix \mathbf{Y}_Ω^o is known as direction of arrival (DOA) estimation.

Due to its connections to line spectral estimation and DOA estimation, studies of the CCS problem have been a long history though frequency estimation has been mainly focused on. Well known conventional methods include periodogram (or beamforming), Capon's beamforming and subspace methods like MUSIC (see [4] for a complete review). Periodogram suffers from the so-called leakage problem and a resolution limit of $\frac{1}{N}$ when all measurements are observed, which makes it difficult to resolve two closely spaced frequencies. The situation becomes even worse with compressive data. Capon's beamforming and MUSIC are *high resolution* methods in the sense that they can break the resolution limit above. However, since they are covariance-based methods they also have difficulties with compressive data unless L is sufficiently large and moreover, they are sensitive to source correlations. With the development of sparse signal representation and later the CS concept, sparse methods have been popular in the last decade which exploit the prior knowledge that the number of frequency components K is small [7]–[21]. However, within the earlier discrete CS framework the frequency domain \mathbb{T} has to be gridded/discretized into a finite set, or equivalently, the frequencies of interest are constrained on a fixed grid, resulting in basis mismatches and a resolution limit [22]. Though modified, off-grid estimation methods [16]–[21] have been implemented to reduce the drawbacks, overall they are still based on gridding of the frequency domain.

The authors are with the School of Electrical and Electronic Engineering, Nanyang Technological University, 639798, Singapore (e-mail: {yangzai, elhxie}@ntu.edu.sg).

Recently, a mathematical theory of super-resolution is introduced by Candès and Fernandez-Granda [23]. They study frequency estimation in the SMV case given the full data \mathbf{Y}^o and propose a gridless sparse method via convex optimization known as the total variation norm or atomic norm technique [24]. In addition, they prove that the frequencies can be recovered with infinite precision in the absence of noise once they are mutually separated by at least $\frac{4}{N}$. This theory was then extended by Tang *et al.* and the authors to the cases with compressive data and/or MMVs, showing that the signal and the frequencies can be exactly recovered with high probability via (convex) atomic norm minimization (ANM) provided $M \geq O(K \ln K \ln N)$ and the same frequency separation condition holds [5], [6], [25]. Many related works have recently emerged and an incomplete list includes [26]–[37]. While the atomic norm techniques eliminate completely basis mismatches of earlier grid-based sparse methods, a major problem is that the frequencies have to be sufficiently separated for successful recovery, prohibiting *high resolution*.¹

In this paper, we attempt to propose a high resolution gridless sparse method for signal and frequency recovery in CCS. Our method is motivated by the formulations and properties of atomic ℓ_0 norm and the atomic norm in [6], [25]. In particular, the atomic ℓ_0 norm directly exploits sparsity and has no resolution limit but is NP hard to compute. To the contrary, as a convex relaxation the atomic norm can be efficiently computed but suffers from a resolution limit as mentioned above. We propose a novel sparse metric and theoretically show that the new metric fills the gap between the atomic ℓ_0 norm and the atomic norm. It approaches the former under appropriate parameter setting and breaks the resolution limit. With the sparse metric we formulate a nonconvex optimization problem for signal and frequency recovery. A locally convergent iterative algorithm is presented to solve the problem. Some further analysis shows that the algorithm iteratively carries out ANM with a sound reweighting strategy which determines preference of frequency selection based on the latest estimate and enhances sparsity and resolution. The resulting algorithm is termed as reweighted atomic-norm minimization (RAM). Extensive numerical simulations are carried out to demonstrate the performance of RAM with application to DOA estimation compared to existing arts.

We note that the idea of reweighted optimization for enhancing sparsity is not new. For example, reweighted ℓ_1 algorithms have been introduced for discrete CS [38]–[40], and reweighted trace minimization for low rank matrix recovery [41], [42]. However, it is unclear how to implement a reweighting strategy in the continuous dictionary setting prior to this paper. Furthermore, besides sparsity we show that the proposed reweighted algorithm enhances resolution which is of great importance in CCS.

Notations used in this paper are as follows. \mathbb{R} and \mathbb{C} denote the sets of real and complex numbers respectively. \mathbb{T} denotes the unit circle $[0, 1]$ by identifying the beginning and the

ending points. Boldface letters are reserved for vectors and matrices. For an integer N , $[N] \triangleq \{1, \dots, N\}$. $|\cdot|$ denotes cardinality of a set, amplitude of a scalar, or determinant of a squared matrix. $\|\cdot\|_1$, $\|\cdot\|_2$ and $\|\cdot\|_F$ denote the ℓ_1 , ℓ_2 and Frobenius norms respectively. \mathbf{A}^T and \mathbf{A}^H are the matrix transpose and conjugate transpose of \mathbf{A} respectively. x_j is the j th entry of a vector \mathbf{x} . Unless otherwise stated, \mathbf{x}_Ω and \mathbf{A}_Ω respectively reserve the entries of \mathbf{x} and the rows of \mathbf{A} indexed by a set Ω . For a vector \mathbf{x} , $\text{diag}(\mathbf{x})$ is a diagonal matrix with \mathbf{x} being its diagonal. $\text{rank}(\cdot)$ denotes the rank and $\text{tr}(\cdot)$ the trace. $\mathbf{A} \geq \mathbf{0}$ means that \mathbf{A} is positive semidefinite (PSD).

The rest of the paper is organized as follows. Section II revisits preliminary gridless sparse methods that motivate this paper. Section III presents a novel sparse metric for signal and frequency recovery. Section IV introduces the RAM algorithm. Section V presents some algorithm implementation methods for accuracy and speed considerations. Section VI provides extensive numerical simulations to demonstrate the performance of RAM. Section VII concludes this paper.

II. PRELIMINARY GRIDLESS SPARSE METHODS BY EXPLOITING SPARSITY

Unless otherwise stated, we assume in this paper that the observed data \mathbf{Y}_Ω^o is contaminated by noise whose energy is bounded by η^2 , where $\eta \geq 0$. It is clear that $\eta = 0$ refers to the noiseless case. The CCS problem is generally ill-posed and solved by exploiting the fact that the number of frequency components K is small—what we call by frequency-sparsity. In particular, we say that \mathbf{Y} is *frequency-sparse* if \mathbf{Y} is composed by only a few frequency components. For signal recovery we seek a *frequency-sparse* candidate \mathbf{Y} which is consistent with the observed data by imposing that $\mathbf{Y} \in \mathcal{S} \triangleq \{\mathbf{Y} \in \mathbb{C}^{N \times L} : \|\mathbf{Y}_\Omega - \mathbf{Y}_\Omega^o\|_F \leq \eta\}$. Therefore, we need to define a sparse metric of \mathbf{Y} first and then optimize the metric over \mathcal{S} for its solution. The frequencies $\{f_k\}$ are estimated by the frequency components composing the solution/estimate of \mathbf{Y} .

A direct sparse metric is the smallest number of frequency components composing \mathbf{Y} , known as the atomic ℓ_0 norm and denoted by $\|\mathbf{Y}\|_{\mathcal{A},0}$ [5], [6], [25]:

$$\|\mathbf{Y}\|_{\mathcal{A},0} = \inf \left\{ \mathcal{K} : \mathbf{Y} = \sum_{k=1}^{\mathcal{K}} \mathbf{a}(f_k) \mathbf{s}_k, f_k \in \mathbb{T} \right\}, \quad (2)$$

where $\mathbf{a}(f) = [1, e^{i2\pi f}, \dots, e^{i2\pi(N-1)f}]^T \in \mathbb{C}^N$ denotes a discrete sinusoid with frequency f , and $\mathbf{s}_k \in \mathbb{C}^{L \times 1}$ is the coefficient vector of the k th sinusoid. According to [5], [6], [25] $\|\mathbf{Y}\|_{\mathcal{A},0}$ can be characterized as the following rank minimization problem:

$$\begin{aligned} \|\mathbf{Y}\|_{\mathcal{A},0} &= \min_{\mathbf{u}} \text{rank}(T(\mathbf{u})), \\ \text{subject to } \text{tr}(\mathbf{Y}^H T(\mathbf{u})^{-1} \mathbf{Y}) &< +\infty, \quad (3) \\ T(\mathbf{u}) &\geq \mathbf{0}. \end{aligned}$$

The first constraint in (3) imposes that \mathbf{Y} lies in the range

¹The frequency separation $\frac{4}{N}$ in theory is sufficient but unnecessary. Empirical studies in [5] suggest that this value can be approximately $\frac{1}{N}$ in the SMV case, while numerical simulations in [25] and other extensive simulations show that it also depends on other factors like K , M and L .

space of a (Hermitian) Toeplitz matrix

$$T(\mathbf{u}) = \begin{bmatrix} u_1 & u_2 & \cdots & u_N \\ u_2^H & u_1 & \cdots & u_{N-1} \\ \vdots & \vdots & \ddots & \vdots \\ u_N^H & u_{N-1}^H & \cdots & u_1 \end{bmatrix} \in \mathbb{C}^{N \times N},$$

where u_j is the j th entry of $\mathbf{u} \in \mathbb{C}^N$. The frequencies composing \mathbf{Y} are encoded in $T(\mathbf{u})$. Once an optimizer of \mathbf{u} , say \mathbf{u}^* , is obtained the frequencies can be retrieved from $T(\mathbf{u}^*)$ according to the Vandermonde decomposition lemma (see, e.g., [4]), which states that any PSD Toeplitz matrix $T(\mathbf{u}^*)$ can be decomposed as

$$T(\mathbf{u}^*) = \sum_{k=1}^{K^*} p_k^* \mathbf{a}(f_k^*) \mathbf{a}(f_k^*)^H, \quad (4)$$

where the order $K^* = \text{rank}(T(\mathbf{u}^*))$ and $p_k^* > 0$ (see a method for realization of the decomposition in [30, Appendix A]). Therefore, by (3) the CCS problem is reformulated as a low rank matrix recovery (LRMR) problem in which the matrix $T(\mathbf{u})$ is Toeplitz structured and positive semidefinite, and its range space contains \mathbf{Y} .

The atomic ℓ_0 norm directly enhances sparsity, however, it is nonconvex and NP-hard to compute according to the rank minimization formulation which encourages computationally feasible alternatives. In this spirit, the atomic (ℓ_1) norm, denoted by $\|\mathbf{Y}\|_{\mathcal{A}}$, is introduced as a convex relaxation of $\|\mathbf{Y}\|_{\mathcal{A},0}$ [5], [6], [25]:

$$\|\mathbf{Y}\|_{\mathcal{A}} = \inf \left\{ \sum_k \|\mathbf{s}_k\|_2 : \mathbf{Y} = \sum_k \mathbf{a}(f_k) \mathbf{s}_k, f_k \in \mathbb{T} \right\}, \quad (5)$$

which can be considered as a continuous version of the $\ell_{2,1}$ norm utilized for joint sparse recovery in discrete CS (see, e.g., [7], [43]). $\|\mathbf{Y}\|_{\mathcal{A}}$ is a norm and has the following semidefinite formulation [5], [6], [25]:

$$\|\mathbf{Y}\|_{\mathcal{A}} = \min_{\mathbf{u}} \frac{1}{2\sqrt{N}} \left[\text{tr}(T(\mathbf{u})) + \text{tr}(\mathbf{Y}^H T(\mathbf{u})^{-1} \mathbf{Y}) \right], \quad (6)$$

subject to $T(\mathbf{u}) \geq \mathbf{0}$.

From the perspective of LRMR, (6) attempts to recover the low rank matrix $T(\mathbf{u})$ by relaxing the pseudo-rank norm in (3) to the nuclear norm or equivalently the trace norm for a PSD matrix. It is worth noting that the positive weight between the two terms in the optimization problem in (6) only alters the optimizer of \mathbf{u} up to a positive scale. Again, the frequencies of interest are encoded in $T(\mathbf{u})$ and can be obtained once the optimization problem is solved within a polynomial time. The atomic norm is advantageous in computation compared to the atomic ℓ_0 norm, however, it suffers from a resolution limit due to the relaxation which is not shared by the latter [5], [23], [25].

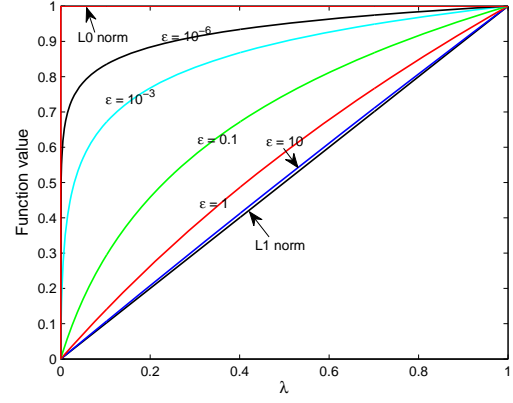


Fig. 1. The sparsity-promoting property of $\mathcal{M}^\epsilon(\cdot)$ with different ϵ . The plotted curves include the ℓ_0 and ℓ_1 norms corresponding to $\|\cdot\|_{\mathcal{A},0}$ and $\|\cdot\|_{\mathcal{A}}$ respectively, and $\ln|\lambda + \epsilon|$ corresponding to $\mathcal{M}^\epsilon(\cdot)$ with $\epsilon = 10, 1, 0.1, 10^{-3}$ and 10^{-6} . $\ln|\lambda + \epsilon|$ is translated and scaled such that it equals 0 and 1 at $\lambda = 0$ and 1 respectively for better illustration.

III. ENHANCING SPARSITY AND RESOLUTION VIA A NOVEL SPARSE METRIC

Inspired by the link between CCS and LRMR demonstrated above, we propose the following sparse metric of \mathbf{Y} :

$$\mathcal{M}^\epsilon(\mathbf{Y}) = \min_{\mathbf{u}} \ln |T(\mathbf{u}) + \epsilon \mathbf{I}| + \text{tr}(\mathbf{Y}^H T(\mathbf{u})^{-1} \mathbf{Y}), \quad (7)$$

subject to $T(\mathbf{u}) \geq \mathbf{0}$,

where $\epsilon > 0$ is a regularization parameter that avoids the first term being $-\infty$ when $T(\mathbf{u})$ is rank deficient. Note that the log-det heuristic $\log|\cdot|$ has been widely used as a smooth surrogate for the rank of a PSD matrix (see, e.g., [41], [42]). From the perspective of LRMR, the atomic ℓ_0 norm minimizes the number of nonzero eigenvalues of $T(\mathbf{u})$ while the atomic ℓ_1 norm minimizes the sum of the eigenvalues. In contrast, the new metric $\mathcal{M}^\epsilon(\mathbf{Y})$ puts penalty on $\sum_{k=1}^N \ln|\lambda_k + \epsilon|$, where $\{\lambda_k\}_{k=1}^N$ denotes the eigenvalues. We plot the function $h(\lambda) = \ln|\lambda + \epsilon|$ with different ϵ 's in Fig. 1 together with the constant function (except at $\lambda = 0$) and the identity function corresponding to the ℓ_0 and ℓ_1 norms respectively, where $h(\lambda)$ is translated and scaled for better illustration without altering its sparsity-enhancing property. Intuitively, $h(\lambda)$ gets close to the ℓ_1 norm for large ϵ while it approaches the ℓ_0 norm as $\epsilon \rightarrow 0$. Therefore, we expect that the new metric $\mathcal{M}^\epsilon(\mathbf{Y})$ bridges $\|\mathbf{Y}\|_{\mathcal{A}}$ and $\|\mathbf{Y}\|_{\mathcal{A},0}$ when ϵ varies from $+\infty$ to 0. Formally, we have the following results.

Theorem 1: Let $\epsilon \rightarrow +\infty$. Then,

$$\mathcal{M}^\epsilon(\mathbf{Y}) - N \ln \epsilon \sim 2\sqrt{N} \|\mathbf{Y}\|_{\mathcal{A}} \epsilon^{-\frac{1}{2}}, \quad (8)$$

i.e., they are equivalent infinitesimals.

Proof: See Appendix A. ■

Theorem 2: Let $\epsilon \rightarrow 0$. Then, we have the following results:

1) If $\|\mathbf{Y}\|_{\mathcal{A},0} \leq N - 1$, then

$$\mathcal{M}^\epsilon(\mathbf{Y}) \sim \left(\|\mathbf{Y}\|_{\mathcal{A},0} - N \right) \ln \frac{1}{\epsilon}, \quad (9)$$

i.e., they are equivalent infinities. Otherwise, $\mathcal{M}^\epsilon(\mathbf{Y})$ is a positive constant depending only on \mathbf{Y} ;

- 2) Let \mathbf{u}_ϵ^* be the optimizer of \mathbf{u} to the optimization problem in (7). Then, the smallest $N - \|\mathbf{Y}\|_{\mathcal{A},0}$ eigenvalues of $T(\mathbf{u}_\epsilon^*)$ are either zero or approach zero as fast as ϵ ;
- 3) For any cluster point of \mathbf{u}_ϵ^* at $\epsilon = 0$, denoted by \mathbf{u}_0^* , there exists an atomic decomposition $\mathbf{Y} = \sum_{k=1}^K \mathbf{a}(f_k) s_k$ of order $K = \|\mathbf{Y}\|_{\mathcal{A},0}$ such that $T(\mathbf{u}_0^*) = \sum_{k=1}^K \|s_k\|_2^2 \mathbf{a}(f_k) \mathbf{a}(f_k)^H$.²

Proof: See Appendix B. ■

Theorem 1 shows that the new metric $\mathcal{M}^\epsilon(\mathbf{Y})$ plays the same role as $\|\mathbf{Y}\|_{\mathcal{A}}$ in the limiting scenario when $\epsilon \rightarrow +\infty$, while Theorem 2 says that it is equivalent to $\|\mathbf{Y}\|_{\mathcal{A},0}$ as $\epsilon \rightarrow 0$. Consequently, it fills the gap between $\|\mathbf{Y}\|_{\mathcal{A}}$ and $\|\mathbf{Y}\|_{\mathcal{A},0}$ and enhances sparsity and resolution compared to $\|\mathbf{Y}\|_{\mathcal{A}}$ as ϵ gets small. Moreover, Theorem 2 characterizes the properties of the optimizer \mathbf{u}_ϵ^* as $\epsilon \rightarrow 0$ including the convergent speed of the smallest $N - K$ eigenvalues and the limiting form of $T(\mathbf{u}^*)$ via the Vandermonde decomposition. In fact, we always observe via simulations that the smallest $N - K$ eigenvalues of $T(\mathbf{u}^*)$ become zero once ϵ is modestly small.

Remark 1: In DOA estimation, a difficult scenario is when the source signals $\{s_k\}_{k=1}^K$ are highly or even completely correlated (the latter is usually called coherent). For example, covariance-based methods like Capon's beamforming and MUSIC cannot produce satisfactory results since a faithful covariance estimate is unavailable. In contrast, the proposed sparse metric is robust to source correlations according to Theorem 2 in which we have not made any assumption for the sources.

Remark 2: According to Theorem 2, the solution $T(\mathbf{u}^*)$ can be interpreted as the data covariance of \mathbf{Y} after removing correlations between the sources.

IV. REWEIGHTED ATOMIC-NORM MINIMIZATION (RAM)

A. A Locally Convergent Iterative Algorithm

With the proposed sparse metric $\mathcal{M}^\epsilon(\mathbf{Y})$, we solve the following optimization problem for signal and frequency recovery:

$$\min_{\mathbf{Y}} \mathcal{M}^\epsilon(\mathbf{Y}), \text{ subject to } \|\mathbf{Y}\boldsymbol{\Omega} - \mathbf{Y}^o\|_F \leq \eta, \quad (10)$$

or equivalently,

$$\begin{aligned} \min_{\mathbf{Y}, \mathbf{u}} \ln |T(\mathbf{u}) + \epsilon \mathbf{I}| + \text{tr}(\mathbf{Y}^H T(\mathbf{u})^{-1} \mathbf{Y}), \\ \text{subject to } T(\mathbf{u}) \geq \mathbf{0} \text{ and } \|\mathbf{Y} - \mathbf{Y}^o\|_F \leq \eta. \end{aligned} \quad (11)$$

Since the log-det term $\ln |T(\mathbf{u}) + \epsilon \mathbf{I}|$ is a concave function of \mathbf{u} , the problem is nonconvex and no efficient algorithms can guarantee to obtain the global optimum. A popular locally convergent approach to minimization of such a concave + convex function is the majorization-maximization (MM) algorithm. Let \mathbf{u}_j denote the j th iterate of the optimization variable

² \mathbf{u}^* is called a cluster point of a vector-valued function $\mathbf{u}(x)$ at $x = x_0$ if there exists a sequence $\{x_n\}_{n=1}^{+\infty}$, $\lim_{n \rightarrow +\infty} x_n = x_0$, satisfying that $\lim_{n \rightarrow +\infty} \mathbf{u}(x_n) \rightarrow \mathbf{u}^*$.

\mathbf{u} . Then, at the $(j+1)$ th iteration we replace $\ln |T(\mathbf{u}) + \epsilon \mathbf{I}|$ by its tangent plane at the current value $\mathbf{u} = \mathbf{u}_j$,

$$\begin{aligned} \ln |T(\mathbf{u}_j) + \epsilon \mathbf{I}| + \text{tr} \left[(T(\mathbf{u}_j) + \epsilon \mathbf{I})^{-1} T(\mathbf{u} - \mathbf{u}_j) \right] \\ = \text{tr} \left[(T(\mathbf{u}_j) + \epsilon \mathbf{I})^{-1} T(\mathbf{u}) \right] + c_j, \end{aligned} \quad (12)$$

where c_j is a constant independent of \mathbf{u} . As a result, the optimization problem at the $(j+1)$ th iteration becomes

$$\begin{aligned} \min_{\mathbf{Y}, \mathbf{u}} \text{tr} \left[(T(\mathbf{u}_j) + \epsilon \mathbf{I})^{-1} T(\mathbf{u}) \right] + \text{tr} \left(\mathbf{Y}^H T(\mathbf{u})^{-1} \mathbf{Y} \right), \\ \text{subject to } T(\mathbf{u}) \geq \mathbf{0} \text{ and } \|\mathbf{Y}\boldsymbol{\Omega} - \mathbf{Y}^o\|_F \leq \eta. \end{aligned} \quad (13)$$

Since $\ln |T(\mathbf{u}) + \epsilon \mathbf{I}|$ is strictly concave in \mathbf{u} , at each iteration its value decreases by an amount greater than the decrease of its tangent plane. It follows that the objective function in (11) monotonically decreases at each iteration and converges to a local minimum.

B. Interpretation as RAM

To interpret the optimization problem in (13), let us define a weighted continuous dictionary

$$\mathcal{A}^w \triangleq \{\mathbf{a}^w(f) = w(f) \mathbf{a}(f) : f \in \mathbb{T}\} \quad (14)$$

w.r.t. the original continuous dictionary $\{\mathbf{a}(f) : f \in \mathbb{T}\}$, where $w(f) \geq 0$ is a weighting function. For $\mathbf{Y} \in \mathbb{C}^{N \times L}$, we define its weighted atomic norm w.r.t. \mathcal{A}^w as its atomic norm induced by \mathcal{A}^w :

$$\begin{aligned} \|\mathbf{Y}\|_{\mathcal{A}^w} \\ \triangleq \inf \left\{ \sum_k \|s_k^w\|_2 : \mathbf{Y} = \sum_k \mathbf{a}^w(f_k) s_k^w, f_k \in \mathbb{T} \right\} \\ = \inf \left\{ \sum_k w(f_k)^{-1} \|s_k\|_2 : \mathbf{Y} = \sum_k \mathbf{a}(f_k) s_k, f_k \in \mathbb{T} \right\}. \end{aligned} \quad (15)$$

According to the definition above, $w(f)$ specifies preference of the atoms $\{\mathbf{a}(f)\}$. To be specific, an atom $\mathbf{a}(f_0)$, $f_0 \in \mathbb{T}$, is more likely selected if $w(f_0)$ is larger. Moreover, the atomic norm is a special case of the weighted atomic norm with a constant weighting function (i.e., without any preference). Similarly to the atomic norm, the proposed weighted atomic norm also admits a semidefinite formulation when assigned an appropriate weighting function, which is stated in the following theorem.

Theorem 3: Suppose that $w(f) = \frac{1}{\sqrt{\mathbf{a}(f)^H \mathbf{W} \mathbf{a}(f)}}$ with $\mathbf{W} \in \mathbb{C}^{N \times N}$. Then,

$$\begin{aligned} \|\mathbf{Y}\|_{\mathcal{A}^w} = \min_{\mathbf{u}} \frac{\sqrt{N}}{2} \text{tr}(\mathbf{W} T(\mathbf{u})) + \frac{1}{2\sqrt{N}} \text{tr}(\mathbf{Y}^H T(\mathbf{u})^{-1} \mathbf{Y}), \\ \text{subject to } T(\mathbf{u}) \geq \mathbf{0}. \end{aligned} \quad (16)$$

Proof: See Appendix C. ■

Let $\mathbf{W}_j = \frac{1}{N} (T(\mathbf{u}_j) + \epsilon \mathbf{I})^{-1}$ and $w_j(f) = \frac{1}{\sqrt{\mathbf{a}(f)^H \mathbf{W}_j \mathbf{a}(f)}}$. By Theorem 3 we can rewrite the

optimization problem in (13) as the following weighted atomic norm minimization problem:

$$\min_{\mathbf{Y}} \|\mathbf{Y}\|_{\mathcal{A}^{w_j}}, \text{ subject to } \|\mathbf{Y}\boldsymbol{\Omega} - \mathbf{Y}_{\boldsymbol{\Omega}}^o\|_F \leq \eta. \quad (17)$$

As a result, the proposed iterative algorithm can be interpreted as reweighted atomic-norm minimization (RAM), where the weighting function is updated based on the latest solution of \mathbf{u} . If we let $w_0(f)$ be a constant function or equivalently, $\mathbf{u}_0 = \mathbf{0}$, such that there is no preference of the atoms at the first iteration, then the first iteration coincides with the ANM. From the second iteration, the preference is defined by the weighting function $w_j(f)$ specified above. Note that $w_j^2(f)$ corresponds to the power spectrum of Capon's beamforming if $T(\mathbf{u}_j)$ is interpreted as the covariance of the noiseless data according to Remark 2 and ϵ as the noise variance. Therefore, the reweighting strategy makes the frequencies around those estimated by the current iteration preferable at the next iteration and thus enhances sparsity. At the same time, the preference leads to finer details of the frequency spectrum in that area and enhances resolution. Empirical evidences will be provided in Section VI. Since the "noise variance" ϵ can be translated as the confidence level in the current estimate, from this perspective we should gradually decrease ϵ and correspondingly increase the confidence in the solution during the algorithm.

V. COMPUTATIONALLY EFFICIENT IMPLEMENTATIONS

A. Optimization by Standard SDP Solver

At each iteration of RAM, we need to solve the SDP in (13) as follows:

$$\begin{aligned} & \min_{\mathbf{u}, \mathbf{X}, \mathbf{Y}} \text{tr}(\mathbf{W}T(\mathbf{u})) + \text{tr}(\mathbf{X}), \\ & \text{subject to } \begin{bmatrix} \mathbf{X} & \mathbf{Y}^H \\ \mathbf{Y} & T(\mathbf{u}) \end{bmatrix} \geq \mathbf{0} \text{ and } \|\mathbf{Y}\boldsymbol{\Omega} - \mathbf{Y}_{\boldsymbol{\Omega}}^o\|_F \leq \eta, \end{aligned} \quad (18)$$

where $\mathbf{W} = (T(\mathbf{u}_j) + \epsilon \mathbf{I})^{-1}$. Its dual problem is given as follows by a standard Lagrangian analysis (see Appendix D):

$$\begin{aligned} & \min_{\mathbf{V}, \mathbf{Z}} 2\eta \|\mathbf{V}\boldsymbol{\Omega}\|_F + 2\Re \text{tr}(\mathbf{Y}_{\boldsymbol{\Omega}}^{oH} \mathbf{V}\boldsymbol{\Omega}), \\ & \text{subject to } \begin{bmatrix} \mathbf{I} & \mathbf{V}^H \\ \mathbf{V} & \mathbf{Z} \end{bmatrix} \geq \mathbf{0}, T^*(\mathbf{Z}) = T^*(\mathbf{W}), \text{ and } \mathbf{V}_{\bar{\boldsymbol{\Omega}}} = \mathbf{0}, \end{aligned} \quad (19)$$

where \Re takes the real part of the argument and $T^*(\cdot)$ denotes the adjoint operator of $T(\cdot)$. We empirically find that the dual problem (19) can be solved more efficiently than the primal problem (18) with a standard SDP solver SDPT3 [44]. It is noted that the optimizer to (18) is given for free via duality when we solve (19). As a result, the reweighted algorithm can be iteratively implemented.

B. A First-order Algorithm via ADMM

A reasonably fast approach for ANM is based on the ADMM [26], [30], [45], which is a first-order algorithm and

guarantees global optimality. To derive the ADMM algorithm, we reformulate the SDP in (18) as follows:

$$\begin{aligned} & \min_{\mathbf{u}, \mathbf{X}, \{\mathbf{Y} : \|\mathbf{Y}\boldsymbol{\Omega} - \mathbf{Y}_{\boldsymbol{\Omega}}^o\|_F \leq \eta\}, \{\mathbf{Q} \geq \mathbf{0}\}} \text{tr}(\mathbf{W}T(\mathbf{u})) + \text{tr}(\mathbf{X}), \\ & \text{subject to } \mathbf{Q} = \begin{bmatrix} \mathbf{X} & \mathbf{Y}^H \\ \mathbf{Y} & T(\mathbf{u}) \end{bmatrix}, \end{aligned} \quad (20)$$

which is very similar to the SDP solved in [30]. Then we can write the augmented Lagrangian function and iteratively update $(\mathbf{u}, \mathbf{X}, \mathbf{Y})$, \mathbf{Q} and the Lagrangian multiplier in closed-form expressions until convergence. We omit the details since all the formulae and derivations are similar to those in [30], to which interested readers are referred. We mention that an eigen-decomposition of a matrix of order $N + L$ (the order of \mathbf{Q}) is required at each iteration. Note that the ADMM converges slowly to an extremely accurate solution while moderate accuracy is typically sufficient in practical applications [45].

C. Dimension Reduction for Large L

The number of measurement vectors L can be large, possibly with $L \gg M$, in DOA estimation, which increases considerably the computational workload. We provide the following result to reduce this number from L to $\text{rank}(\mathbf{Y}_{\boldsymbol{\Omega}}^o) \leq \min(L, M)$.

Proposition 1: Let $r = \text{rank}(\mathbf{Y}_{\boldsymbol{\Omega}}^o) \leq \min(L, M)$. Find a unitary matrix $\mathbf{Q} \in \mathbb{C}^{L \times L}$ (for example, by QR decomposition) such that $\mathbf{Y}_{\boldsymbol{\Omega}}^o \mathbf{Q} = \mathbf{Y}_{\boldsymbol{\Omega}}^o [\mathbf{Q}_1 \quad \mathbf{Q}_2] = [\mathbf{Y}_{\boldsymbol{\Omega}}^o \mathbf{Q}_1 \quad \mathbf{0}]$, where $\mathbf{Q}_1 \in \mathbb{C}^{L \times r}$. If we make substitutions $\mathbf{Y}_{\boldsymbol{\Omega}}^o \rightarrow \mathbf{Y}_{\boldsymbol{\Omega}}^o \mathbf{Q}_1$ and $\mathbf{Y} \in \mathbb{C}^{N \times L} \rightarrow \mathbf{Z} \in \mathbb{C}^{N \times r}$ in (13) and denote by $(\mathbf{Z}^*, \mathbf{u}^*)$ the optimizer to the resulting optimization problem, then the optimizer to (13) is given by $(\mathbf{Z}^* \mathbf{Q}_1^H, \mathbf{u}^*)$. The same result holds with the nonconvex optimization problem in (10).

Proof: See Appendix E. \blacksquare

Remark 3: If only the frequency estimation is of interest, e.g., in DOA estimation, we can replace $\mathbf{Y}_{\boldsymbol{\Omega}}^o \mathbf{Q}_1$ by $(\mathbf{Y}_{\boldsymbol{\Omega}}^o \mathbf{Y}_{\boldsymbol{\Omega}}^{oH})^{\frac{1}{2}}$ (in fact, any matrix $\tilde{\mathbf{Y}}$ satisfying that $\tilde{\mathbf{Y}} \tilde{\mathbf{Y}}^H = \mathbf{Y}_{\boldsymbol{\Omega}}^o \mathbf{Y}_{\boldsymbol{\Omega}}^{oH}$) to obtain the same solution of \mathbf{u} .

Remark 4: With a similar proof, the dimension reduction technique in Proposition 1 can be extended to a more general linear model with observations expressed by $\Phi \mathbf{Y}^o$ plus noise, where Φ denotes a sensing matrix. Also, it can be applied to conventional discrete dictionary models, in which, for example, the $\ell_{2,p}$ norm, $0 < p \leq 1$, needs to be optimized. As a direct application, we can replace the SVD procedure in ℓ_1 -SVD [7], which carries out dimension reduction with approximations given the source number K , by an exact QR decomposition process without the knowledge of K .

By Proposition 1, when $L > M$ we can reduce the order of the PSD matrix in (18) [and (19), (20)] from $N + L$ to $N + r \leq N + M$. Therefore, the resulting problem dimension depends only on M and N . Both the implementations of RAM above are reasonably fast when M and N are small though they may not possess good scalability, especially for SDPT3. An application at hand is DOA estimation in which the array size M and length N are typically small (on the order of 10)

though L can be a few hundred or even more. Note also that the dimension reduction technique takes $O(M^2L)$ flops in DOA estimation according to Remark 3. Extensive numerical simulations will be provided in Section VI to demonstrate usefulness of our method.

D. Remarks on Algorithm Implementation

According to the discussions in Section IV-B, we can always start with $\mathbf{u}_0 = \mathbf{0}$ and then the first iteration coincides with the ANM. When L is modestly large, we can also implement a weighting function in the first iteration inspired by Capon's beamforming for faster convergence (see an example in Section VI-D). Moreover, we should gradually decrease ϵ during the algorithm to increase confidence in the obtained solution. This is like an aggressive continuation strategy in which we attempt to solve the nonconvex optimization problem in (10) at decreasing values of ϵ , while for speed consideration we only solve each problem approximately at each ϵ and go to the next value with a warm start. The convergence of the reweighted algorithm is retained if we fix ϵ when it is sufficiently small. Note also that ϵ cannot be too small in practical implementation for calculation of the matrix inversion. In the ADMM implementation, we can further accelerate the computations by adopting loose convergence criteria in the first few iterations of the reweighted algorithm. Finally, it is noted that there exists a trade off between the algorithm performance and the computational speed.

VI. NUMERICAL SIMULATIONS

A. Implementation Details of RAM

In RAM, we first scale the measurements and the noise such that $\|\mathbf{Y}_\Omega\|_F^2 = M$ (the noise energy becomes $\eta'^2 = \frac{M\eta^2}{\|\mathbf{Y}_\Omega\|_F^2}$) and compensate the recovery afterwards. We start with $\mathbf{u}_0 = \mathbf{0}$ and $\epsilon = 1$ as default. We halve ϵ when beginning a new iteration until $\epsilon = \frac{1}{2^{10}}$ or $\epsilon < \frac{\eta'^2}{10}$. When $\eta = 0$ we terminate RAM if the relative change (in the Frobenius norm) of the solution \mathbf{Y}^* at two consecutive iterations is less than 1×10^{-6} or the maximum number of iterations, set to 20, is reached. All simulations are carried out in Matlab v.8.1.0 on a PC with a Windows 7 system and a 3.4 GHz CPU.

B. An Illustrative Example

We provide a simple example in this subsection to illustrate the iterative process of RAM. In particular, we consider a sparse frequency spectrum consisting of $K = 5$ spikes located at 0.1, 0.108, 0.125, 0.2 and 0.5. We randomly generate the complex amplitudes and randomly select $M = 30$ samples among $N = 64$ consecutive time-space measurements, with $L = 1$. Then, we run the RAM algorithm to reconstruct the frequency spectrum from the samples. Note that the first three frequencies are mutually separated by only about $\frac{0.51}{N}$ and $\frac{1.09}{N}$. Implemented with SDPT3 the RAM algorithm converges in four iterations. We plot the simulation results in Fig. 2, where the first subfigure presents variation of the eigenvalues of $T(\mathbf{u}^*)$ during the iterations, the second row presents the recovered spectra of the first three iterations, and the last row

plots the weighting functions used in the first three iterations to produce the spectra. Note that the first iteration, which exploits a constant weighting function and coincides with the ANM, can detect a rough area where the first three spikes are located but cannot accurately determine their locations and number. In the second iteration, a weighting function is implemented based on the previous estimate to provide preference of the frequencies around those produced in the first iteration. As a result, the third spike is identified while the first two are still not. Following from the same reweighting process, all the frequencies are correctly determined in the next iteration and the algorithm converges after that. It is worth noting that $T(\mathbf{u}^*)$ becomes rank-5 and the remaining eigenvalues become zero (within numerical precision) after three iterations, where $\epsilon = 0.25$. Finally, we report that the relative mean squared error (MSE) of signal recovery improves during the iterations from 1.28×10^{-4} to 2.01×10^{-7} , 3.16×10^{-19} and 3.01×10^{-21} . Each iteration takes about 1.7s.

C. Sparsity-Separation Phase Transition

In this subsection, we study the success rate of RAM in signal and frequency recovery compared to ANM. In particular, we fix $N = 64$ and $M = 30$ with the sampling index set Ω being generated uniformly at random. We vary the duo (K, Δ_f) and at each combination we randomly generate K frequencies such that they are mutually separated by at least Δ_f . We randomly generate the amplitudes $\{s_{kt}\}$ independently and identically from a standard complex normal distribution. After obtaining the noiseless samples, we carry out signal reconstruction and frequency recovery using ANM and RAM, both implemented by SDPT3. The recovery is called successful if both the relative MSE of signal recovery and the MSE of frequency recovery are less than 1×10^{-12} . At each combination (K, Δ_f) , the success rate is measured over 20 Monte Carlo runs.

We plot the success rates of ANM and RAM with $L = 1$ in Fig. 3, where it is shown that successful recovery can be obtained with more ease with a smaller K and a larger frequency separation Δ_f , leading to a phase transition in the sparsity-separation domain. By comparing the two images, we see that RAM significantly enlarges the success phase and hence enhances sparsity and resolution. It is worth noting that the phase transitions of both ANM and RAM are not sharp. One reason is that, a set of *well separated* frequencies can be possibly generated at a small value of Δ_f since we only control that the frequencies are separated by *at least* Δ_f . It is also observed that RAM tends to converge in less iterations with a smaller K and a larger Δ_f .

We also consider the MMV case with $L = 5$. The success rates of ANM and RAM are presented in Fig. 4. Again, remarkable improvement is obtained by the proposed RAM compared to ANM. In fact, we did not find a single failure in our simulation whenever $K \leq 20$ and $\Delta_f \geq \frac{0.3}{N}$. By comparing the results in Figs. 3 and 4, it can be observed that improved signal and frequency recovery performance can be obtained by increasing L , which has been shown in [6], [25].

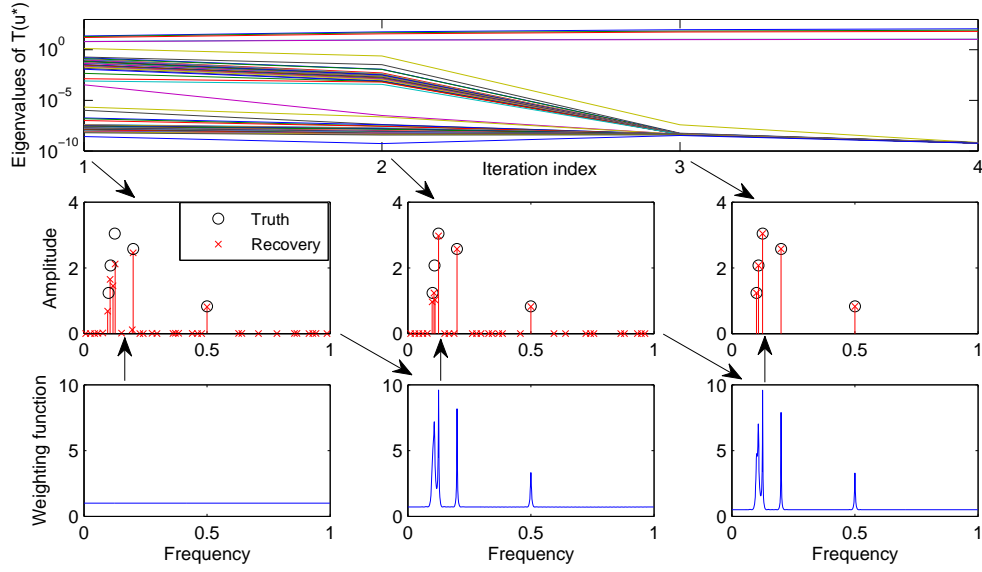


Fig. 2. An illustrative example of RAM. Some settings include $N = 64$, $M = 30$, $K = 5$ with frequencies located at 0.1, 0.108, 0.125, 0.2 and 0.5. The first row presents variation of eigenvalues of $T(u^*)$ w.r.t. the iteration index. Only 5 eigenvalues remain nonzero (within numerical precision) after 3 iterations. The second row presents the recovered spectra of the first 3 iterations. The last row plots the weighting functions used in the first 3 iterations to produce the spectra. Note that the first iteration coincides with the ANM with a constant weighting function.

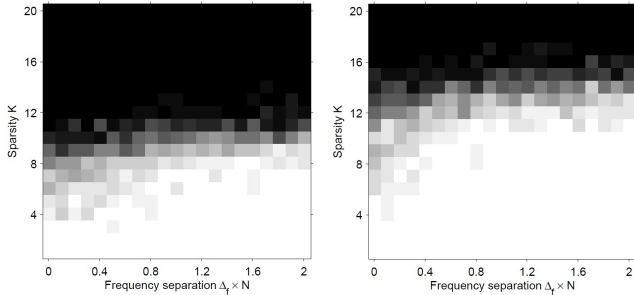


Fig. 3. Sparsity-separation phase transitions of ANM (left) and RAM (right) with $L = 1$, $N = 64$ and $M = 30$. The grayscale images present the success rates, where white and black colors indicate complete success and complete failure, respectively.

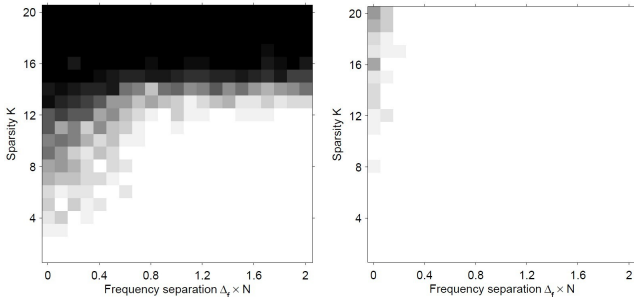


Fig. 4. Sparsity-separation phase transitions of ANM (left) and RAM (right) with $L = 5$, $N = 64$ and $M = 30$. The grayscale images present the success rates, where white and black colors indicate complete success and complete failure, respectively.

D. Application to DOA Estimation

We apply the proposed RAM method to DOA estimation. In particular, we consider a 10-element SLA array with sensors' positions indexed by $\Omega = \{1, 2, 5, 6, 8, 12, 15, 17, 19, 20\}$, where the distance between the first two sensors is half the wavelength. Hence, we have that $N = 20$ and $M = 10$. We consider that $K = 4$ narrowband sources impinge on the sensor array from directions corresponding to frequencies 0.1, 0.11, 0.2 and 0.5, and powers 10, 10, 3 and 1, respectively. Therefore, it is challenging to separate the first two sources which are separated by only $\frac{0.2}{N}$. We consider both cases of uncorrelated and correlated sources. In the latter case, sources 1 and 3 are set to be coherent (completely correlated). Assume that $L = 200$ data snapshots are collected which are corrupted by i.i.d. Gaussian noise of unit variance. In our simulation, both ANM and RAM are implemented using both SDPT3 and ADMM. A nontrivial weighting function is implemented in the first iteration of RAM with $W = \Gamma_{\Omega}^T \left(\frac{1}{L} Y_{\Omega}^o Y_{\Omega}^{oH} + \epsilon I \right)^{-1} \Gamma_{\Omega}$, where $\Gamma_{\Omega} \in \{0, 1\}^{M \times N}$ has 1 in the j th row only at the Ω_j th position. The weighting function corresponds to Capon's beamforming with $\frac{1}{L} Y_{\Omega}^o Y_{\Omega}^{oH}$ being the data covariance and ϵ a regularization parameter. We terminate RAM within maximally 10 iterations. We consider MUSIC and ANM for comparison. We assume that the noise variance $\sigma^2 = 1$ is given for ANM and RAM and the source number K is provided for MUSIC. We set $\eta^2 = \left(ML + 2\sqrt{ML} \right) \sigma^2$ (mean + twice standard deviation) to upper bound the noise energy with high probability in ANM and RAM.

Our simulation results of 100 Monte Carlo runs are presented in Fig. 5 (only the first 20 runs are presented for MUSIC for better illustration). In the absence of source correlations,

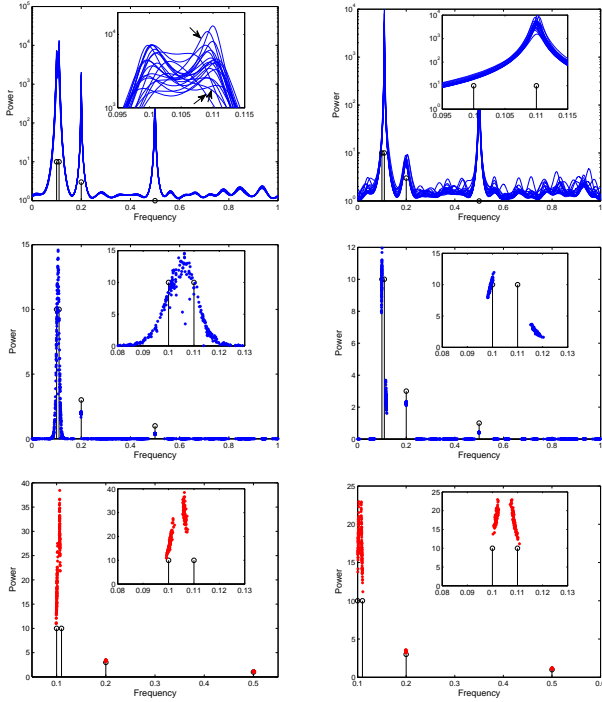


Fig. 5. Results of MUSIC (top), ANM (middle) and RAM (bottom) for frequency spectrum estimation with uncorrelated (left) and correlated (right) sources in 100 Monte Carlo runs. Sources 1 and 3 are coherent in the case of correlated sources. The area around the first two sources are zoomed in in each subfigure. Only results of the first 20 runs are presented for MUSIC for the purpose of better illustration.

MUSIC has satisfactory performance in most scenarios. However, its power spectrum exhibits only a single peak around the first two sources (i.e., the two sources cannot be separated) in at least 3 out of the first 20 runs (indicated by the arrows). Moreover, MUSIC is sensitive to source correlations and cannot detect source 1 when it is coherent with source 3. ANM cannot separate the first two sources in the uncorrelated source case and always produces many spurious sources. In contrast, the proposed RAM always correctly detects 4 sources near the true locations, demonstrating its capabilities in enhancing sparsity and resolution. It is interesting to note that the first two sources tend to merge together in RAM. In fact, when the noise is heavier, we may only detect a single source around the first two and 3 sources in total, which is of course reasonable. Note also that the results of ANM and RAM presented in Fig. 5 are produced by the ADMM implementations, while those by SDPT3 are very similar and omitted. In computational speed, the SDPT3 versions of ANM and RAM take 0.87s and 7.31s on average, respectively, while these numbers are decreased to 0.20s and 2.65s for the ADMM ones.

VII. CONCLUSION

In this paper, we studied the signal and frequency recovery problem in CCS. Motivated by its connection to the topic of LRMR, we proposed reweighted atomic-norm minimization (RAM) for enhancing sparsity and resolution compared to currently prominent atomic norm minimization (ANM) and validated its performance via numerical simulations. As a

byproduct, we have established a framework for applying LRMR techniques to CCS. In future studies, we may try other methods for matrix rank minimization in the literature and propose more computationally efficient algorithms for CCS.

APPENDIX

A. Proof of Theorem 1

Note that

$$\begin{aligned} \mathcal{M}^\epsilon(\mathbf{Y}) - N \ln \epsilon \\ = \min_{\mathbf{u}} \ln |\epsilon^{-1} T(\mathbf{u}) + \mathbf{I}| + \text{tr}(\mathbf{Y}^H T(\mathbf{u})^{-1} \mathbf{Y}), \quad (21) \\ \text{subject to } T(\mathbf{u}) \geq \mathbf{0}. \end{aligned}$$

Let

$$\begin{aligned} \mathbf{u}^* = \arg \min_{\mathbf{u}} \text{tr}(T(\mathbf{u})) + \text{tr}(\mathbf{Y}^H T(\mathbf{u})^{-1} \mathbf{Y}), \quad (22) \\ \text{subject to } T(\mathbf{u}) \geq \mathbf{0}. \end{aligned}$$

Then, according to (6) we have that

$$\text{tr}(T(\mathbf{u}^*)) + \text{tr}(\mathbf{Y}^H T(\mathbf{u}^*)^{-1} \mathbf{Y}) = 2\sqrt{N} \|\mathbf{Y}\|_{\mathcal{A}}. \quad (23)$$

Consider the value of the objective function in (21) at $\mathbf{u} = \epsilon^{\frac{1}{2}} \mathbf{u}^*$. It holds that

$$\begin{aligned} \mathcal{M}^\epsilon(\mathbf{Y}) - N \ln \epsilon \\ \leq \ln |\epsilon^{-\frac{1}{2}} T(\mathbf{u}^*) + \mathbf{I}| + \text{tr}(\mathbf{Y}^H T(\mathbf{u}^*)^{-1} \mathbf{Y}) \epsilon^{-\frac{1}{2}} \\ = \text{tr}(T(\mathbf{u}^*)) \epsilon^{-\frac{1}{2}} + o(\epsilon^{-\frac{1}{2}}) + \text{tr}(\mathbf{Y}^H T(\mathbf{u}^*)^{-1} \mathbf{Y}) \epsilon^{-\frac{1}{2}} \\ = 2\sqrt{N} \|\mathbf{Y}\|_{\mathcal{A}} \epsilon^{-\frac{1}{2}} + o(\epsilon^{-\frac{1}{2}}). \quad (24) \end{aligned}$$

On the other hand, we denote by \mathbf{u}_ϵ^* the optimizer to the optimization problem in (21). We first argue that $\text{tr}(T(\mathbf{u}_\epsilon^*)) \epsilon^{-1} = o(1)$. Otherwise, by (21) $\mathcal{M}^\epsilon(\mathbf{Y}) - N \ln \epsilon \geq \ln |\epsilon^{-1} T(\mathbf{u}_\epsilon^*) + \mathbf{I}|$ is not an infinitesimal, contradicting (24). Therefore,

$$\begin{aligned} \mathcal{M}^\epsilon(\mathbf{Y}) - N \ln \epsilon \\ = \ln |\epsilon^{-1} T(\mathbf{u}_\epsilon^*) + \mathbf{I}| + \text{tr}(\mathbf{Y}^H T(\mathbf{u}_\epsilon^*)^{-1} \mathbf{Y}) \\ = \text{tr}(T(\mathbf{u}_\epsilon^*)) \epsilon^{-1} + o(\text{tr}(T(\mathbf{u}_\epsilon^*)) \epsilon^{-1}) \\ + \text{tr}(\mathbf{Y}^H T(\mathbf{u}_\epsilon^*)^{-1} \mathbf{Y}) \\ = \left[\text{tr}(T(\mathbf{u}_\epsilon^*)) + \text{tr}(\epsilon^{\frac{1}{2}} \mathbf{Y}^H T(\mathbf{u}_\epsilon^*)^{-1} \mathbf{Y} \epsilon^{\frac{1}{2}}) \right] \epsilon^{-1} \\ + o(\text{tr}(T(\mathbf{u}_\epsilon^*)) \epsilon^{-1}) \\ \geq 2\sqrt{N} \|\epsilon^{\frac{1}{2}} \mathbf{Y}\|_{\mathcal{A}} \epsilon^{-1} + o(\text{tr}(T(\mathbf{u}_\epsilon^*)) \epsilon^{-1}) \\ = 2\sqrt{N} \|\mathbf{Y}\|_{\mathcal{A}} \epsilon^{-\frac{1}{2}} + o(\text{tr}(T(\mathbf{u}_\epsilon^*)) \epsilon^{-1}). \quad (25) \end{aligned}$$

Combining (24) and the second equality in (25) yields that $\text{tr}(T(\mathbf{u}_\epsilon^*)) \epsilon^{-1} = O(\epsilon^{-\frac{1}{2}})$. Then, the last equality in (25) gives that

$$\mathcal{M}^\epsilon(\mathbf{Y}) - N \ln \epsilon \geq 2\sqrt{N} \|\mathbf{Y}\|_{\mathcal{A}} \epsilon^{-\frac{1}{2}} + o(\epsilon^{-\frac{1}{2}}). \quad (26)$$

The conclusion is finally drawn by combining (24) and (26).

B. Proof of Theorem 2

Our proof is given in four steps. Let $K = \|\mathbf{Y}\|_{\mathcal{A},0}$, and $\{\lambda_{\epsilon,k}\}_{k=1}^N$ be the eigenvalues of $T(\mathbf{u}_\epsilon^*)$ that are sorted descendingly. In *Step 1*, we attempt to show that there exists a constant $c > 0$ such that $\lambda_{\epsilon,K} \geq c$ holds uniformly for $\epsilon \in (0, 1]$. Let $T(\mathbf{u}_\epsilon^*) = \sum_{k=1}^N \lambda_{\epsilon,k} \mathbf{q}_{\epsilon,k} \mathbf{q}_{\epsilon,k}^H = \mathbf{Q} \text{diag}(\lambda_{\epsilon,1}, \dots, \lambda_{\epsilon,N}) \mathbf{Q}^H$ be the eigen-decomposition, where $\mathbf{q}_{\epsilon,k}$ is the k th column of \mathbf{Q} and $\mathbf{Q}\mathbf{Q}^H = \mathbf{I}$. Then,

$$\mathcal{M}^\epsilon(\mathbf{Y}) = \sum_{k=1}^N \ln |\lambda_{\epsilon,k} + \epsilon| + \sum_{k=1}^N \frac{\bar{p}_{\epsilon,k}}{\lambda_{\epsilon,k}}, \quad (27)$$

where $\bar{p}_{\epsilon,k} \triangleq \|\mathbf{q}_{\epsilon,k}^H \mathbf{Y}\|_2^2$. According to the optimality of \mathbf{u}_ϵ^* , the right hand side of the equation above obtains its minimum at $\lambda_{\epsilon,k}$. Since its derivative at $\lambda_{\epsilon,k}$ equals $\frac{1}{\lambda_{\epsilon,k} + \epsilon} - \frac{\bar{p}_{\epsilon,k}}{\lambda_{\epsilon,k}^2}$, we have that

$$\bar{p}_{\epsilon,k} = \begin{cases} 0, & \text{if } \lambda_{\epsilon,k} = 0, \\ \frac{\lambda_{\epsilon,k}^2}{\lambda_{\epsilon,k} + \epsilon} \in (\lambda_{\epsilon,k} - \epsilon, \lambda_{\epsilon,k}), & \text{otherwise.} \end{cases} \quad (28)$$

Therefore,

$$\text{tr}(T(\mathbf{u}_\epsilon^*)) = \sum_{k=1}^N \lambda_{\epsilon,k} < \sum_{k=1}^N \bar{p}_{\epsilon,k} + N\epsilon = \frac{1}{L} \|\mathbf{Y}\|_F^2 + N \quad (29)$$

provided that $\epsilon \leq 1$. That means, \mathbf{u}_ϵ^* and $\{\lambda_{\epsilon,k}\}$ are bounded.

On the other hand, let $T(\mathbf{u}_\epsilon^*) = \sum_{k=1}^N p_{\epsilon,k} \mathbf{a}(f_{\epsilon,k}) \mathbf{a}(f_{\epsilon,k})^H = \mathbf{A} \mathbf{P} \mathbf{A}^H$ be the (informally written) Vandermonde decomposition, where $\{p_{\epsilon,k}\}_{k=1}^N$ are sorted descendingly and only the first $K_\epsilon^* = \text{rank}(T(\mathbf{u}_\epsilon^*))$ elements are nonzero. Then, \mathbf{Y} is in the range space of \mathbf{A} with $\mathbf{Y} = \mathbf{A} \mathbf{S}$ for some \mathbf{S} . Let $\mathbf{s}_{\epsilon,k}$ be its k th row of \mathbf{S} . Then we have

$$\mathcal{M}^\epsilon(\mathbf{Y}) = \ln |\mathbf{A} \mathbf{P} \mathbf{A}^H + \epsilon \mathbf{I}| + \text{tr}(\mathbf{S}^H \mathbf{P}^{-1} \mathbf{S}). \quad (30)$$

According to the optimality of \mathbf{u}_ϵ^* , the right hand side of the equation above obtains its minimum at $p_{\epsilon,k}$. As a result, its derivative at $p_{\epsilon,k}$ equals 0, i.e.,

$$\mathbf{a}(f_{\epsilon,k})^H (\mathbf{A} \mathbf{P} \mathbf{A}^H + \epsilon \mathbf{I})^{-1} \mathbf{a}(f_{\epsilon,k}) - \frac{\|\mathbf{s}_{\epsilon,k}\|_2^2}{p_{\epsilon,k}^2} = 0, \quad (31)$$

and so $p_{\epsilon,k} > \|\mathbf{s}_{\epsilon,k}\|_2^2$ since

$$\mathbf{a}(f_{\epsilon,k})^H (\mathbf{A} \mathbf{P} \mathbf{A}^H + \epsilon \mathbf{I})^{-1} \mathbf{a}(f_{\epsilon,k}) < p_{\epsilon,k}^{-1} \quad (32)$$

provided that $\epsilon > 0$. Since $\text{tr}(T(\mathbf{u}_\epsilon^*)) = N \sum_{k=1}^N p_{\epsilon,k}$ and that \mathbf{u}_ϵ^* is bounded as shown previously, $\{p_{\epsilon,k}\}$ and $\{\mathbf{s}_{\epsilon,k}\}$ are bounded.

We now prove that $\lambda_{\epsilon,K} \geq c$ for some constant c . Otherwise, for any $c_j = \frac{1}{j}$, $j = 1, 2, \dots$, there exists $\epsilon_j \in (0, 1]$ such that $\lambda_{\epsilon_j,K} < c_j = \frac{1}{j}$. Since the sequence $\left\{ \left(\mathbf{u}_{\epsilon_j}^*, \lambda_{\epsilon_j,k}, \mathbf{q}_{\epsilon_j,k}, p_{\epsilon_j,k}, f_{\epsilon_j,k}, \mathbf{s}_{\epsilon_j,k} \right) \right\}_{j=1}^\infty$ is bounded, there must exist a convergent subsequence. Without loss of generality, we assume that the sequence is convergent itself and denote by $(\mathbf{u}^*, \lambda_k, \mathbf{q}_k, p_k, f_k, \mathbf{s}_k)$ the limit point. Since $\lambda_{K^*} =$

$\lim_{j \rightarrow \infty} \lambda_{\epsilon_j,K} = 0$, we have $\lambda_k = 0$ for all $k = K+1, \dots, N$. It follows that

$$T(\mathbf{u}^*) = \sum_{k=1}^{K-1} \lambda_k \mathbf{q}_k \mathbf{q}_k^H \quad (33)$$

and $\text{rank}(T(\mathbf{u}^*)) \leq K-1$. As a result, at most $K-1$ f_k 's are retained in the decomposition $T(\mathbf{u}^*) = \sum_{k=1}^N p_k \mathbf{a}(f_k) \mathbf{a}(f_k)^H$ if we remove repetitive f_k 's and those with $p_k = 0$. Note that $\mathbf{s}_k = \mathbf{0}$ if $p_k = 0$ since we have shown that $p_{\epsilon,k} \geq \|\mathbf{s}_{\epsilon,k}\|_2^2$. Then, by a similar operation we can reduce the order of the decomposition $\mathbf{Y} = \sum_{k=1}^N \mathbf{a}(f_k) \mathbf{s}_k$ to maximally $K-1$, i.e., we obtain an atomic decomposition of order at most $K-1$, which contradicts that $\|\mathbf{Y}\|_{\mathcal{A},0} = K$ and leads to the conclusion.

In *Step 2* we prove the first part of the theorem. According to (27) and the bound $\lambda_{\epsilon,K} \geq c$ shown in *Step 1*, we have that

$$\begin{aligned} \mathcal{M}^\epsilon(\mathbf{Y}) &= \sum_{k=1}^N \ln |\lambda_{\epsilon,k} + \epsilon| + \sum_{k=1}^N \frac{\bar{p}_{\epsilon,k}}{\lambda_{\epsilon,k}} \\ &\geq \sum_{k=1}^N \ln |\lambda_{\epsilon,k} + \epsilon| \\ &\geq (N-K) \ln \epsilon + K \ln c. \end{aligned} \quad (34)$$

On the other hand, we consider an atomic decomposition of \mathbf{Y} of order K , $\mathbf{Y} = \sum_{k=1}^K \mathbf{a}(f_k) \mathbf{s}_k$. Let $T(\mathbf{u}) = \sum_{k=1}^K \|\mathbf{s}_k\|_2^2 \mathbf{a}(f_k) \mathbf{a}(f_k)^H$, and $\{\lambda_k\}_{k=1}^K$ be the K nonzero eigenvalues of $T(\mathbf{u})$ which are constants independent of ϵ . Then, provided $\epsilon \leq 1$ we have that

$$\begin{aligned} \mathcal{M}^\epsilon(\mathbf{Y}) &\leq (N-K) \ln \epsilon + \sum_{k=1}^K \ln |\lambda_k + \epsilon| + K \\ &\leq (N-K) \ln \epsilon + \sum_{k=1}^K \ln |\lambda_k + 1| + K. \end{aligned} \quad (35)$$

Combining (34) and (35), it yields that $\mathcal{M}^\epsilon(\mathbf{Y}) \sim (N-K) \ln \epsilon$ as $\epsilon \rightarrow 0$.

In *Step 3* we prove the second part of the theorem. Based on (34) and (35) we have that

$$\begin{aligned} (N-K) \ln \epsilon + c_1 &\leq \mathcal{M}^\epsilon(\mathbf{Y}) \\ &\geq \sum_{k=K+1}^N \ln |\lambda_{\epsilon,k} + \epsilon| + \sum_{k=1}^K \ln |\lambda_{\epsilon,k} + \epsilon| \\ &\geq (N-K) \ln \epsilon + \sum_{k=K+1}^N \ln \left| \frac{\lambda_{\epsilon,k}}{\epsilon} + 1 \right| + c_2, \end{aligned} \quad (36)$$

where c_1 and c_2 are constants independent of ϵ . Therefore, it must hold that

$$\ln \left| \frac{\lambda_{\epsilon,K+1}}{\epsilon} + 1 \right| \leq \sum_{k=K+1}^N \ln \left| \frac{\lambda_{\epsilon,k}}{\epsilon} + 1 \right| \leq c_1 - c_2. \quad (37)$$

It follows that

$$0 \leq \lambda_{\epsilon,N} \leq \dots \leq \lambda_{\epsilon,K+1} \leq (e^{c_1-c_2} - 1) \epsilon, \quad (38)$$

i.e., $\lambda_{\epsilon,k} = O(\epsilon)$, $k = K+1, \dots, N$.

Finally, we show the last part of the theorem. For any cluster point \mathbf{u}_0^* of \mathbf{u}_ϵ^* at $\epsilon = 0$, there exists a sequence $\{\mathbf{u}_{\epsilon_j}^*\}_{j=1}^\infty$ converging to \mathbf{u}_0^* , where $\epsilon_j \rightarrow 0$ as $j \rightarrow \infty$. It must hold that $\text{rank}(T(\mathbf{u}_0^*)) = K$ since the smallest $N - K$ eigenvalues of $T(\mathbf{u}_{\epsilon_j}^*)$ approach 0. Moreover, the eigen-decomposition of $T(\mathbf{u}_{\epsilon_j}^*)$ converge to that of $T(\mathbf{u}_0^*)$, where again we denote their eigenvalues by $\{\lambda_{\epsilon_j,k}\}$ and $\{\lambda_k\}$ respectively and use the other notations similarly. Then, according to (28) we have that $\bar{p}_{\epsilon_j,k} = \frac{\lambda_{\epsilon_j,k}^2}{\lambda_{\epsilon_j,k} + \epsilon} \rightarrow \lambda_k = \bar{p}_k$, as $j \rightarrow \infty$. Therefore,

$$\text{tr}(\mathbf{Y}^H T(\mathbf{u}_0^*)^{-1} \mathbf{Y}) = \sum_{k=1}^K \frac{\bar{p}_k}{\lambda_k} = K. \quad (39)$$

On the other hand, we similarly write the Vandermonde decomposition of $T(\mathbf{u}_\epsilon^*)$ and let $T(\mathbf{u}_0^*) = \sum_{k=1}^K p_k \mathbf{a}(f_k) \mathbf{a}(f_k)^H$, with $\mathbf{Y} = \sum_{k=1}^K \mathbf{a}(f_k) \mathbf{s}_k$. It is easy to show that $p_k \geq \|\mathbf{s}_k\|_2^2$ based on the inequality $p_{\epsilon,k} > \|\mathbf{s}_{\epsilon,k}\|_2^2$, though $p_{\epsilon,k}$ and $\mathbf{s}_{\epsilon,k}$ do not necessarily converge to p_k and \mathbf{s}_k (consider the case where an accumulation point of $\{f_{\epsilon_j,1}, \dots, f_{\epsilon_j,N}\}_{j=1}^\infty$ contains identical elements). Then,

$$\text{tr}(\mathbf{Y}^H T(\mathbf{u}_0^*)^{-1} \mathbf{Y}) = \sum_{k=1}^K \frac{\|\mathbf{s}_k\|_2^2}{p_k} \leq K, \quad (40)$$

where the equality holds iff $p_k = \|\mathbf{s}_k\|_2^2$. So, we complete the proof.

C. Proof of Theorem 3

The conclusion is a direct result of the following equalities:

$$\begin{aligned} & \min_{\mathbf{u}} \frac{\sqrt{N}}{2} \text{tr}(\mathbf{W}T(\mathbf{u})) + \frac{1}{2\sqrt{N}} \text{tr}(\mathbf{Y}^H T(\mathbf{u})^{-1} \mathbf{Y}), \\ & \text{subject to } T(\mathbf{u}) \geq \mathbf{0} \\ & = \min_{f_k, p_k} \frac{\sqrt{N}}{2} \text{tr}(\mathbf{W}\mathbf{R}) + \frac{1}{2\sqrt{N}} \text{tr}(\mathbf{Y}^H \mathbf{R}^{-1} \mathbf{Y}), \\ & \text{subject to } \mathbf{R} = \sum_k p_k \mathbf{a}(f_k) \mathbf{a}(f_k)^H \\ & = \min_{f_k, p_k, \mathbf{s}_k} \frac{\sqrt{N}}{2} \sum_k \mathbf{a}(f_k)^H \mathbf{W} \mathbf{a}(f_k) p_k + \frac{1}{2\sqrt{N}} \sum_k \|\mathbf{s}_k\|_2^2 p_k^{-1}, \\ & \text{subject to } \mathbf{Y} = \sum_k \mathbf{a}(f_k) \mathbf{s}_k \\ & = \min_{f_k, p_k, \mathbf{s}_k} \frac{\sqrt{N}}{2} \sum_k w(f_k)^{-2} p_k + \frac{1}{2\sqrt{N}} \sum_k \|\mathbf{s}_k\|_2^2 p_k^{-1}, \\ & \text{subject to } \mathbf{Y} = \sum_k \mathbf{a}(f_k) \mathbf{s}_k \\ & = \min_{f_k, \mathbf{s}_k} \sum_k w(f_k)^{-1} \|\mathbf{s}_k\|_2, \text{ subject to } \mathbf{Y} = \sum_k \mathbf{a}(f_k) \mathbf{s}_k \\ & = \|\mathbf{Y}\|_{\mathcal{A}^w}, \end{aligned} \quad (41)$$

where the first equality applies the Vandermonde decomposition, and the second follows the equality (see [25])

$$\begin{aligned} & \text{tr}(\mathbf{Y}^H \mathbf{R}^{-1} \mathbf{Y}) \\ & = \min_{f_k, \mathbf{s}_k} \sum_k \|\mathbf{s}_k\|_2^2 p_k^{-1}, \text{ subject to } \mathbf{Y} = \sum_k \mathbf{a}(f_k) \mathbf{s}_k \end{aligned} \quad (42)$$

given the expression of \mathbf{R} in (41).

D. Lagrangian Analysis of the Dual Problem (19)

Let $\Lambda = \begin{bmatrix} \mathbf{U} & \mathbf{V}^H \\ \mathbf{V} & \mathbf{Z} \end{bmatrix} \geq \mathbf{0}$. The Lagrangian function of (18) is given as follows:

$$\begin{aligned} \mathcal{L}(\mathbf{u}, \mathbf{X}, \mathbf{Y}, \Lambda, \lambda) & = \text{tr}(\mathbf{W}T(\mathbf{u})) + \text{tr}(\mathbf{X}) - \text{tr}\left(\begin{bmatrix} \mathbf{X} & \mathbf{Y}^H \\ \mathbf{Y} & T(\mathbf{u}) \end{bmatrix} \Lambda\right) \\ & \quad + \lambda (\|\mathbf{Y}\Omega - \mathbf{Y}_\Omega^o\|_F^2 - \eta^2) \\ & = \text{tr}[(\mathbf{W} - \mathbf{Z})T(\mathbf{u})] + \text{tr}[(\mathbf{I} - \mathbf{U})\mathbf{X}] - 2\Re\text{tr}(\mathbf{Y}_\Omega^H \mathbf{V} \bar{\Omega}) \\ & \quad + \lambda \|\mathbf{Y}\Omega - \mathbf{Y}_\Omega^o - \lambda^{-1} \mathbf{V}\Omega\|_F^2 - \lambda^{-1} \|\mathbf{V}\Omega\|_F^2 - \lambda \eta^2 \\ & \quad - 2\Re\text{tr}(\mathbf{Y}_\Omega^{oH} \mathbf{V}\Omega). \end{aligned}$$

Minimizing \mathcal{L} with respect to $(\mathbf{u}, \mathbf{X}, \mathbf{Y})$ gives the dual objective which equals $-\lambda^{-1} \|\mathbf{V}\Omega\|_F^2 - \lambda \eta^2 - 2\Re\text{tr}(\mathbf{Y}_\Omega^H \mathbf{V}\Omega)$, if

$$T^*(\mathbf{W} - \mathbf{Z}) = \mathbf{0}, \quad \mathbf{U} = \mathbf{I}, \text{ and } \mathbf{V}\bar{\Omega} = \mathbf{0},$$

or $-\infty$, otherwise. Therefore, we obtain the dual problem in (19) by noticing that

$$\lambda^{-1} \|\mathbf{V}\Omega\|_F^2 + \lambda \eta^2 \leq 2\eta \|\mathbf{V}\Omega\|_F.$$

E. Proof of Proposition 1

Regarding (13) and (11) we consider the following optimization problem:

$$\min_{\mathbf{Y}} \text{tr}(\mathbf{Y}^H \mathbf{C} \mathbf{Y}), \text{ subject to } \|\mathbf{Y}\Omega - \mathbf{Y}_\Omega^o\|_F^2 \leq \eta^2, \quad (43)$$

where $\mathbf{C} \geq \mathbf{0}$ is fixed. We replace the optimization variable \mathbf{Y} by $\mathbf{Z} = \mathbf{Y}\mathbf{Q}$. Since \mathbf{Q} is a unitary matrix, the problem becomes

and equivalently,

$$\begin{aligned} & \min_{\mathbf{Z}_1, \mathbf{Z}_2} \text{tr}(\mathbf{Z}_1^H \mathbf{C} \mathbf{Z}_1) + \text{tr}(\mathbf{Z}_2^H \mathbf{C} \mathbf{Z}_2), \\ & \text{subject to } \|\mathbf{Z}_1\Omega - \mathbf{Y}_\Omega^o \mathbf{Q}_1\|_F^2 + \|\mathbf{Z}_2\Omega\|_F^2 \leq \eta^2, \end{aligned}$$

where $\mathbf{Z}_j = \mathbf{Y}\mathbf{Q}_j$, $j = 1, 2$. Denote the optimizer by $(\mathbf{Z}_1^*, \mathbf{Z}_2^*)$. It is obvious that $\mathbf{Z}_2^* = \mathbf{0}$ since $\text{tr}(\mathbf{Z}_2^H \mathbf{C} \mathbf{Z}_2) \geq 0$. Then the problem becomes

$$\min_{\mathbf{Z}_1} \text{tr}(\mathbf{Z}_1^H \mathbf{C} \mathbf{Z}_1), \text{ subject to } \|\mathbf{Z}_1\Omega - \mathbf{Y}_\Omega^o \mathbf{Q}_1\|_F^2 \leq \eta^2,$$

which is a dimension reduced version of (43) and has the same optimal function value. Moreover, given $\mathbf{Z}^* = [\mathbf{Z}_1^* \quad \mathbf{0}]$ we have the optimizer to (43) $\mathbf{Y}^* = \mathbf{Z}^* \mathbf{Q}^H = \mathbf{Z}_1^* \mathbf{Q}_1^H$. Now the conclusion can be easily drawn.

REFERENCES

- [1] E. Candès, "Compressive sampling," in *Proceedings of the International Congress of Mathematicians*, vol. 3, 2006, pp. 1433–1452.
- [2] D. Donoho, "Compressed sensing," *IEEE Transactions on Information Theory*, vol. 52, no. 4, pp. 1289–1306, 2006.
- [3] H. Krim and M. Viberg, "Two decades of array signal processing research: The parametric approach," *IEEE Signal Processing Magazine*, vol. 13, no. 4, pp. 67–94, 1996.
- [4] P. Stoica and R. L. Moses, *Spectral analysis of signals*. Pearson/Prentice Hall Upper Saddle River, NJ, 2005.
- [5] G. Tang, B. N. Bhaskar, P. Shah, and B. Recht, "Compressed sensing off the grid," *IEEE Transactions on Information Theory*, vol. 59, no. 11, pp. 7465–7490, 2013.
- [6] Z. Yang and L. Xie, "Continuous compressed sensing with a single or multiple measurement vectors," in *IEEE Workshop on Statistical Signal Processing (SSP)*, 2014, pp. 308–311.
- [7] D. Malioutov, M. Cetin, and A. Willsky, "A sparse signal reconstruction perspective for source localization with sensor arrays," *IEEE Transactions on Signal Processing*, vol. 53, no. 8, pp. 3010–3022, 2005.
- [8] M. Hyder and K. Mahata, "Direction-of-arrival estimation using a mixed $\ell_{2,0}$ norm approximation," *IEEE Transactions on Signal Processing*, vol. 58, no. 9, pp. 4646–4655, 2010.
- [9] P. Stoica, P. Babu, and J. Li, "New method of sparse parameter estimation in separable models and its use for spectral analysis of irregularly sampled data," *IEEE Transactions on Signal Processing*, vol. 59, no. 1, pp. 35–47, 2011.
- [10] —, "SPICE: A sparse covariance-based estimation method for array processing," *IEEE Transactions on Signal Processing*, vol. 59, no. 2, pp. 629–638, 2011.
- [11] X. Wei, Y. Yuan, and Q. Ling, "DOA estimation using a greedy block coordinate descent algorithm," *IEEE Transactions on Signal Processing*, vol. 60, no. 12, pp. 6382–6394, 2012.
- [12] A. Fannjiang and W. Liao, "Coherence pattern-guided compressive sensing with unresolved grids," *SIAM Journal on Imaging Sciences*, vol. 5, no. 1, pp. 179–202, 2012.
- [13] N. Hu, Z. Ye, X. Xu, and M. Bao, "DOA estimation for sparse array via sparse signal reconstruction," *IEEE Transactions on Aerospace and Electronic Systems*, vol. 49, no. 2, pp. 760–773, 2013.
- [14] M. F. Duarte and R. G. Baraniuk, "Spectral compressive sensing," *Applied and Computational Harmonic Analysis*, vol. 35, no. 1, pp. 111–129, 2013.
- [15] Z. Liu, Z. Huang, and Y. Zhou, "Sparsity-inducing direction finding for narrowband and wideband signals based on array covariance vectors," *IEEE Transactions on Wireless Communications*, vol. 12, no. 8, pp. 3896–3907, 2013.
- [16] L. Hu, Z. Shi, J. Zhou, and Q. Fu, "Compressed sensing of complex sinusoids: An approach based on dictionary refinement," *IEEE Transactions on Signal Processing*, vol. 60, no. 7, pp. 3809–3822, 2012.
- [17] Z. Yang, C. Zhang, and L. Xie, "Robustly stable signal recovery in compressed sensing with structured matrix perturbation," *IEEE Transactions on Signal Processing*, vol. 60, no. 9, pp. 4658–4671, 2012.
- [18] Z. Yang, L. Xie, and C. Zhang, "Off-grid direction of arrival estimation using sparse Bayesian inference," *IEEE Transactions on Signal Processing*, vol. 61, no. 1, pp. 38–43, 2013.
- [19] L. Hu, J. Zhou, Z. Shi, and Q. Fu, "A fast and accurate reconstruction algorithm for compressed sensing of complex sinusoids," *IEEE Transactions on Signal Processing*, vol. 61, no. 22, pp. 5744–5754, 2013.
- [20] C. Austin, J. Ash, and R. Moses, "Dynamic dictionary algorithms for model order and parameter estimation," *IEEE Transactions on Signal Processing*, vol. 61, no. 20, pp. 5117–5130, 2013.
- [21] Z. Tan, P. Yang, and A. Nehorai, "Joint sparse recovery method for compressed sensing with structured dictionary mismatch," *IEEE Transactions on Signal Processing*, DOI: 10.1109/TSP.2014.2343940, 2014.
- [22] Y. Chi, L. Scharf, A. Pezeshki, and A. Calderbank, "Sensitivity to basis mismatch in compressed sensing," *IEEE Transactions on Signal Processing*, vol. 59, no. 5, pp. 2182–2195, 2011.
- [23] E. J. Candès and C. Fernandez-Granda, "Towards a mathematical theory of super-resolution," *Communications on Pure and Applied Mathematics*, vol. 67, no. 6, pp. 906–956, 2014.
- [24] V. Chandrasekaran, B. Recht, P. A. Parrilo, and A. S. Willsky, "The convex geometry of linear inverse problems," *Foundations of Computational Mathematics*, vol. 12, no. 6, pp. 805–849, 2012.
- [25] Z. Yang and L. Xie, "Exact joint sparse frequency recovery via optimization methods," Available online at <http://arxiv.org/abs/1405.6585>, 2014.
- [26] B. N. Bhaskar, G. Tang, and B. Recht, "Atomic norm denoising with applications to line spectral estimation," *IEEE Transactions on Signal Processing*, vol. 61, no. 23, pp. 5987–5999, 2013.
- [27] E. J. Candès and C. Fernandez-Granda, "Super-resolution from noisy data," *Journal of Fourier Analysis and Applications*, DOI: 10.1007/s00041-013-9292-3, 2013.
- [28] G. Tang, B. N. Bhaskar, and B. Recht, "Near minimax line spectral estimation," in *47th Annual Conference on Information Sciences and Systems (CISS)*. IEEE, 2013, pp. 1–6.
- [29] Z. Yang, L. Xie, and C. Zhang, "A discretization-free sparse and parametric approach for linear array signal processing," *IEEE Transactions on Signal Processing*, vol. 62, no. 19, pp. 4959–4973, 2014.
- [30] Z. Yang and L. Xie, "On gridless sparse methods for line spectral estimation from complete and incomplete data," Available online at <http://arxiv.org/abs/1407.2490>, 2014.
- [31] J.-M. Azais, Y. De Castro, and F. Gamboa, "Spike detection from inaccurate samplings," *Applied and Computational Harmonic Analysis*, DOI: 10.1016/j.acha.2014.03.004, 2014.
- [32] L. Condat and A. Hirabayashi, "Cadzow denoising upgraded: A new projection method for the recovery of dirac pulses from noisy linear measurements," Available online at <http://hal.archives-ouvertes.fr/docs/00/84/79/84/PDF/double.pdf>, 2013.
- [33] Y. Chen and Y. Chi, "Robust spectral compressed sensing via structured matrix completion," *IEEE Transactions on Information Theory*, DOI: 10.1109/TIT.2014.2343623, 2014.
- [34] Z. Tan, Y. C. Eldar, and A. Nehorai, "Direction of arrival estimation using co-prime arrays: A super resolution viewpoint," Available online at <http://arxiv.org/abs/1312.7793>, 2013.
- [35] K. V. Mishra, M. Cho, A. Kruger, and W. Xu, "Off-the-grid spectral compressed sensing with prior information," in *IEEE International Conference on Acoustics, Speech and Signal Processing (ICASSP)*, 2014, pp. 1010–1014.
- [36] Z. Lu, R. Ying, S. Jiang, Z. Zhang, P. Liu, and W. Yu, "Distributed compressed sensing off the grid," Available online at <http://arxiv.org/abs/1407.3064>, 2014.
- [37] Y. Chi, "Joint sparsity recovery for spectral compressed sensing," in *IEEE International Conference on Acoustics, Speech and Signal Processing (ICASSP)*, 2014, pp. 3938–3942.
- [38] M. S. Lobo, M. Fazel, and S. Boyd, "Portfolio optimization with linear and fixed transaction costs," *Annals of Operations Research*, vol. 152, no. 1, pp. 341–365, 2007.
- [39] E. J. Candès, M. B. Wakin, and S. P. Boyd, "Enhancing sparsity by reweighted ℓ_1 minimization," *Journal of Fourier Analysis and Applications*, vol. 14, no. 5–6, pp. 877–905, 2008.
- [40] D. Wipf and S. Nagarajan, "Iterative reweighted ℓ_1 and ℓ_2 methods for finding sparse solutions," *IEEE Journal of Selected Topics in Signal Processing*, vol. 4, no. 2, pp. 317–329, 2010.
- [41] M. Fazel, H. Hindi, and S. P. Boyd, "Log-det heuristic for matrix rank minimization with applications to Hankel and Euclidean distance matrices," in *American Control Conference*, vol. 3. IEEE, 2003, pp. 2156–2162.
- [42] K. Mohan and M. Fazel, "Iterative reweighted algorithms for matrix rank minimization," *The Journal of Machine Learning Research*, vol. 13, no. 1, pp. 3441–3473, 2012.
- [43] E. Van Den Berg and M. Friedlander, "Theoretical and empirical results for recovery from multiple measurements," *IEEE Transactions on Information Theory*, vol. 56, no. 5, pp. 2516–2527, 2010.
- [44] K.-C. Toh, M. J. Todd, and R. H. Tütüncü, "SDPT3—a MATLAB software package for semidefinite programming, version 1.3," *Optimization Methods and Software*, vol. 11, no. 1–4, pp. 545–581, 1999.
- [45] S. Boyd, N. Parikh, E. Chu, B. Peleato, and J. Eckstein, "Distributed optimization and statistical learning via the alternating direction method of multipliers," *Foundations and Trends® in Machine Learning*, vol. 3, no. 1, pp. 1–122, 2011.